INTERNATIONAL JOURNAL OF OPTIMIZATION IN CIVIL ENGINEERING
Int. J. Optim. Civil Eng., 2021; 11(4): 631-646

OPTIMUM LEVEL OF DISCRETE WAVELET DECOMPOSITION FOR DYNAMIC ANALYSIS OF HYDRAULIC STRUCTURES

S. Shabankhah[1], A. Heidari[2*, †] and R. Kamgar[3]
[1]*Master of Science Student, Shahrekord University, Shahrekord, Iran*
[2]*Associate Professor of Civil Engineering, Shahrekord University, Shahrekord, Iran*
[3]*Associate Professor of Civil Engineering, Shahrekord University, Shahrekord, Iran*

ABSTRACT

Seismic analysis of structures is a process for estimating the response of structures subjected to earthquakes. For this purpose, the earthquake is analyzed using the wavelet theory. In this paper, the primary signal of the earthquake is decomposed through a discrete wavelet transform, and their corresponding response spectrum is obtained. Then, the percentage difference between the decomposed signals and the main one is computed. Therefore, for different earthquakes, a comparison between the response spectrum is studied in various types of dams. The acceleration, velocity, and displacement responses are computed and compared to achieve an appropriate level of decomposition, which can be used instead of the primary signal. Therefore, the decomposition process leads to attaining acceptable accuracy as well as low computational cost. The investigation revealed that the acceleration, velocity, and displacement responses spectrum are suitable up to the third level of decomposition for the small and medium dams, whereas for large dams, up to the fifth level of decomposition is suitable.

Keywords: seismic analysis; discrete wavelet transform; response spectrum; dam.

Received: 28 May 2021; Accepted: 24 September 2021

1. INTRODUCTION

Structures are subjected to time-varying seismic forces during an earthquake, producing time-dependent displacements and internal stresses. Seismic analysis techniques can calculate the Strong Ground Motion parameters (SGMs) and the response spectrum. The static analysis method should not be used for the ultimate design of any structures. In contrast, earthquake loading is the governing case, particularly for regions with a high

[*]Corresponding author: Department of Civil Engineering, Shahrekord University, Shahrekord, Iran
[†]E-mail address: heidari@sku.ac.ir (A. Heidari)

probability of severe earthquakes (e.g., soils type III and IV). This fact can be held for irregular structures. Besides, the time history analysis should be used in retrofitting structures against earthquakes and for seismic damaged-based design. Therefore, the response parameters are used to control structural damage in the performance-based seismic design of structures. Some important parameters are base shear, story drift, spectral acceleration, spectral displacement, and story displacement [1]. Also, the Peak Ground Acceleration (PGA), Peak Ground Velocity (PGV), and peak ground displacement (PGD) are the ground motion amplitude characteristics that can be obtained from the accelerograms.

The importance of PGA is related to the development of seismic zoning maps and the construction of the design Response Spectrum (RS), which is used in earthquake-resistant construction rules [2]. Effective PGAs are needed in the early stages of project development since they can be used as a starting point for preliminary seismic designs and evaluations [3]. The PGA is used in the regression analysis model to determine the intensity of an earthquake [4]. The PGV plays a vital role in the problem of velocity RS to produce a family of curves called maximum relative velocity RS [5]. PGV has been widely used in risk analysis and performance-based design in sensitive seismic zones [6]. PGD has been commonly employed to predict and formulate the ground-motion prediction equation for a considered region [7]. PGD is one of the factors governing the seismic demand in the time history analysis, performance-based seismic design [8], the displacement hazard analysis [9], development of the structural collapse prediction models [10], and the earthquake resistant design of structures [11]. For some non-stationary time-series signals, the low Signal to the Noise Ratio (SNR) values are entirely covered by seismic noise.

Moreover, the low and high-frequency noises often exist in the accelerograms and affect the properties of the SGM parameters. As noises affect the parameters of SGM, the appropriate processing should be applied to the accelerograms before using it. Accordingly, denoising is a significant component of earthquake engineering and seismic hazard studies [12]. Frequency processing of accelerograms is an advanced technique for filtering seismic noise [13]. The ground acceleration value needs to be transformed into a frequency domain to remove the noise using the frequency filtering technique. The low-frequency signals travel longer distances and transmit to an even more profound zone of the earth’s subsurface.

Moreover, the high-frequency signals are often represented by short wiggles and can be reconstructed through data denoising. Fourier Transform (FT) is widely used to process accelerogram when the signal is considered stationary. However, as the accelerograms are highly non-stationary, wavelet processing came to researchers' attention. The Fourier transform is considered as a starting point. It also is an alternative representation of a signal in the frequency domain.

On the other hand, the Wavelet Transform (WT) is the best representation for the signal analysis in the time and frequency domain [14, 15]. There are different WTs, such as Discrete Wavelet Transform (DWT) [16-18] and Continuous Wavelet Transform (CWT) [19]. WT decomposes the accelerogram in various frequency levels and analyzes the signal based on time-scale transformation [20]. Therefore, decomposing an accelerogram using WT will clearly distinguish the noise and signal characteristics. Wavelet analysis enables one to represent a function in terms of a set of fundamental functions called mother wavelets

(Symlet, Coiflet, Debeuches, Haar, etc.), localized in both time and space. WT-based processing has been used to reach the optimal design of structures subjected to earthquake loadings [20]. Heidari et al. used WT to estimate the parameters of SGM based on the decomposition of the primary signal [21, 22].

This paper uses the DWT to obtain an appropriate decomposition level for the time history analysis of dam structures. Inhere, three different types of dams are considered, and the spectral dynamic analysis is applied to reach the optimum level of decomposition. It should be noted that there are different optimization methods used in engineering problems [23-26]. These methods can find optimal solutions for engineering problems. Researchers combined the wavelet transform with optimization algorithms to find the optimal solutions for engineering problems [27-29].

2. WAVELET TRANSFORM

In the following section, two types of WT (DWT and CWT) are discussed.

2.1 Continuous wavelet transform

Any oscillating function with zero mean can be a mother wavelet. The wavelet transform of $f \in L^2(R)$ at time u and scale s is a convolution of the mother function $\psi \in L^2(R)$ with the function$f \in L^2(R)$:

$$Wf(u,s) = \int_{-\infty}^{\infty} f(t) \left(\frac{1}{\sqrt{s}}\right) \psi^* \left(\frac{t-u}{s}\right) dt = f * \overline{\psi_s}\,(u) \tag{1}$$

By applying the Parseval formula, Eq. (1) can also be written as:

$$Wf(u,s) = \int_{-\infty}^{\infty} f(t)\, {\psi_{u,s}}^*(t) dt = \frac{1}{2\pi} \int_{-\infty}^{\infty} \hat{f}\,(\omega) \widehat{{\psi_{u,s}}^*}(\omega) d\omega \tag{2}$$

where, Wf(u,s) is the wavelet coefficients, f(t) is the signal function, $\hat{f}(\omega)$ is the signal spectrum. The wavelet coefficients are determined by the signal and its spectrum in the time-frequency region, where the energy of $\widehat{{\psi_{u,s}}^*}$ and ${\psi_{u,s}}^*$ is concentrated. Since it has a zero average, a wavelet coefficient $Wf(u,s)$ measures the variation of f in the adjacent of u, which its size is proportional to s. U transmission parameter is related to the location of the wavelet function as it is shifted along with the signal. In contrast, the scale parameter of s is defined as the inverse of frequency. The main CWT drawback is its performance in computing for both scale and translation, which turns this transform into a redundant one. Therefore, a discretization of the scale and translation variables was introduced.

2.2 Discrete wavelet transform

The discretization of CWT leads to the Discrete Wavelet Transform in the time-frequency plane, which contributes to decomposing discrete-time signals. The following result at each

decomposition level consists of two coefficients: approximate coefficients and detail coefficients. The former coefficients are obtained by low-pass filtering of the input sequence, followed by down-sampling. The latter ones are obtained by high-pass filtering of the input sequence, followed by down-sampling. The sequence of coefficients approximation provides the input for the next iteration. Each decomposition level corresponds to a specific resolution.

The Discrete Wavelet Transform has two main features: the wavelet mother $\boldsymbol{\psi}$ and the number of decomposition levels. Discrete wavelets can be scaled and translated into distinct steps, which its representation shows in the following:

$$\psi_{j,n} = \frac{1}{\sqrt{2^j}}\left(\frac{t - 2^j n}{2^j}\right) \tag{3}$$

where *j* is the scale factor, and *n* is the translation index.

Classical DWT is not shift-invariant, meaning that the DWT of a translated version of the signal is not the same as the identical translation of DWT of the original one.

The Stationary Wavelet Transform overcomes the absence of translation invariance of the DWT. The SWT, also known as the Undecimated Discrete Wavelet Transform, is a time-redundant version of standard DWT.

Unlike the DWT, which down-samples the approximation coefficients and detail coefficients at each decomposition level, no down-sampling is performed in the case of SWT. This difference means that the approximation coefficients and the detailed one at each level have the same length as the initial signal. Therefore an increased number of coefficients is determined at each scale leading to more accurate localization of signal features, whereas the filters are up-sampled at each level.

The SWT has the translation-invariance or shift-invariance feature. Therefore, the SWT provides a more significant amount of information about the transformed signal when compared to DWT. A more substantial amount of data is essential when statistical methods are used for analyzing the wavelet coefficients. The shift-invariant property is vital in feature-extraction applications, denoising, as well as detection. The SWT can be implemented using the Shensa algorithm.

2.3 Stationary wavelet transform

Another way to perform a multiresolution analysis is using the Shensa algorithm, which corresponds to the computation of Stationary Wavelet Transform. The decomposition tree is represented in Fig. 1.

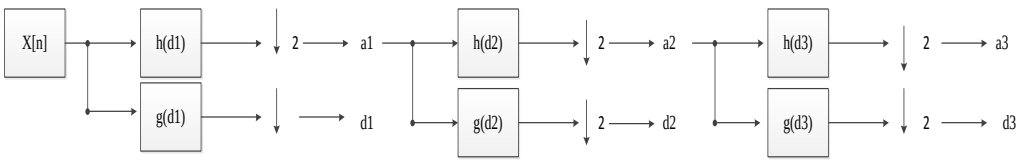

Figure 1. Systems for the Stationary Wavelet Transform (SWT)

In this case, dampers are avoided, but different low-pass filters ($h_{d_1}, h_{d_2}, h_{d_3}$) and high-pass ones ($g_{d_1}, g_{d_2}, g_{d_3}$) are used at each iteration. Each level filters are up-sampled versions

of previous ones.

Therefore the differences between SWT and DWT are that the signal is never down-sampled, while the filters are up-sampled at each level in the case of SWT. The SWT is a translation-invariant because all the filters composting scheme is linear time-invariant systems (see Fig. 1).

3. MODELING PROCEDURE

The fundamental period is a common criterion describing the behavior of building subjected to seismic loads. So, it is used to determine the requirements of a structure due to a given seismic input. First of all, the fundamental period of the small, medium, and large dams should be defined, respectively. Then, the response spectrum of the main earthquake is compared with the decomposed levels in the desired range.

Dams are classified into three types of small, medium, and large dams based on height and capability (see Table 1).

Table 1: Classification of dams

Type	Maximum capability (m^3)	Height (m)
Small	61674 to 1.233×10^6	7.62 to 12.192
Median	1.233×10^6 <cap< 61674000	12.192<h<30.48
Large	>61674000	>30.48

For calculating the fundamental period of dams, based on ASCE7-10 [30], the following formula is used:

$$T_a = 0.0488(h_n)^{0.75} \tag{1}$$

where $\boldsymbol{h_n}$ shows the structure height from ground level, and $\boldsymbol{T_a}$ presents the fundamental period of the structure. Table 2 shows the period range of the dam resulting from Table 1 and Eqs. (1-4).

Table 2: The period range of dams

Dam Type	Period (*Sec*)
Small	0.22-0.318
Median	0.318-0.633
Large	>0.633

In this section, the earthquakes are decomposed with DWT, and then, the difference of the primary earthquake response spectrum is compared with decomposed levels ones.

4. RESULTS

In this section, earthquake data is decomposed into five levels by DWT. Each decomposition

level has two parts, namely a Detailed coefficient and an Approximate coefficient, which result from high-pass filters and low-pass filters, respectively. The approximate coefficient is the base of comparing features with the main signal because it has a similar length and property to the main one. Earthquake properties are extracted from SeismoSignal software based on acceleration, velocity, and displacement. SeismoSignal can compute Strong Ground Motion Parameres based on various damping ratios. Here, the linear response spectrum is considered. The reason for transferring data from SeismoSignal into Matlab is that the former software analyzes the data based on Fourier Transform. In contrast, the latter is used to analyze the data based on Wavelet transform.

In this paper, the damping ratio is considered to be equal to 5%. The selected earthquake is "**ElCentro,"** which occurred on the United States and Mexico border in 1940.

The decomposition process continued up to the fifth level. It yielded results in the form of graphs such as acceleration-period, velocity-period, displacement-period, acceleration-frequency, velocity-frequency, and displacement-frequency, which has been compared with the initial signal at %5 damping ratio.

4.1 Acceleration-period

Fig. 2 shows the acceleration-period comparison of 5 levels of response spectrum decomposition with the original one. The X-axis shows the period(second) of the earthquake, and the Y-axis shows the acceleration (m/sec^2) of the response spectrum.

Table 2 is used to categorize the dam. Also, the R1, R2, R3, R4, and R5 show level one to five response spectrum.

Fig. 2 demonstrates the acceleration differences of the decomposed response spectrum with the main one in three types of the small, medium, and large dams, respectively. As the graph shows, the first three levels of decomposition can replace the primary response spectrum. This is because of the slight and acceptable difference between the results in small and medium dams. This conclusion can be a bit different for large dams. The fifth level can not be suitable for optimizing due to its relatively considerable disparity. On the other hand, all other decomposition levels of the accelerations (i.e., up to the fourth level) can be used as the original signal alternative for design and optimization purposes.

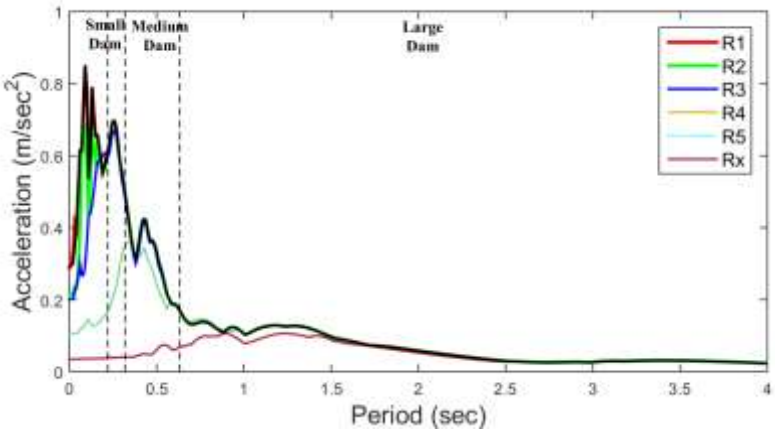

Figure 2. The acceleration response spectrum of the ElCentro earthquake for 5 % damping ratio

The mean percentage difference between each decomposition level and the original signal is calculated in the small dams to study these types of dams. The results are shown in Table 3. The term 'Mpd' stands for Mean Percentage Difference, and the numbers one to five show the corresponding decomposition level. Analyzing the table reflects that the first three levels have a slight difference (under 5 percent), and the remaining levels (i.e., four and five) have more than 50 percent disparity.

Table 3: The mean response difference percentage for the small dams (0.22-0.318 *sec*)

Decomposition level	Value
Mpd1 (%)	0.03
Mpd2 (%)	0.50
Mpd3 (%)	2.93
Mpd4 (%)	57.25
Mpd5 (%)	93.47

A similar analysis is performed for the medium dams, and the results are shown in Table 4. In this type of dam, the results follow a similar pattern in the first three levels, and their percentage differences are under 5 percent. However, the measures of the fourth and fifth levels are less than the corresponding values for the small dams.

Table 4: The mean response difference percentage for the median dams (0.318-0.633 *sec*)

Decomposition level	Value
Mpd1 (%)	0.06
Mpd2 (%)	0.19
Mpd3 (%)	1.78
Mpd4 (%)	13.22
Mpd5 (%)	78.01

This process has a different result for large dams, which is shown in Table 5. Four decomposition levels have a percentage difference of less than 10 percent and can be replaced for optimization and design. However, the fifth level is not suitable due to its considerable disparity.

Comparing these dams reflects that large dams have more flexibility and adaptability with the decomposition levels of accelerations.

Table 5: The mean response difference percentage for the large dams (>0.633 *sec*)

Decomposition level	Value
Mpd1 (%)	0.06
Mpd2 (%)	0.20
Mpd3 (%)	0.31
Mpd4 (%)	1.36
Mpd5 (%)	8.65

The percentage difference of each point between the decomposition level and the main

one is computed at the next step. This can represent a more in-depth analysis to reach the optimum alternative level as the primary function. The term 'pd' indicates the percentage difference, and the following number represents the decomposition level.

As shown in Fig. 3, the percentage difference in the short and medium dams is appropriate up to the third level, and its value is under 10 percent. In the large dams, the maximum value of the difference is 8.9% which is for the fourth level of decomposition. It shows that this decomposition level is suitable.

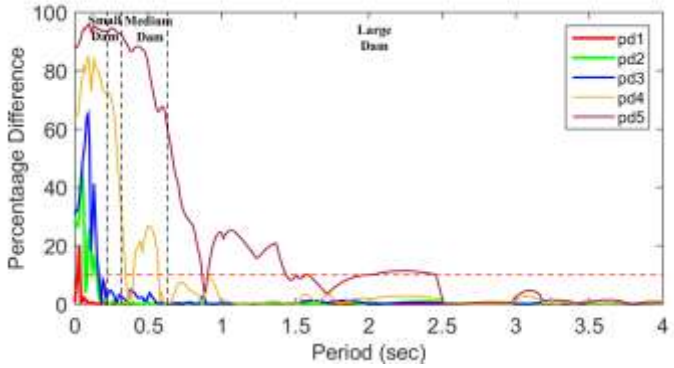

Figure 3. Percentage error for a point-by-point comparison with the original signal

Here, the percentage of cumulative difference for each level of decomposition is made to test the accuracy of the previous two steps (see Fig. 4). The term 't0' is a demonstrator of the first level, which sum with zero. The term 't1' results from the cumulative sum of 't0' with the percentage differences at level 2, and subsequently, 't2' is the result of the cumulative sum of 't1' with the percentage difference at level 3.

There are four horizontal lines in the graph to control the maximum error limit in the value of cumulative differences. These lines are 10, 20, 30, and 40 percent, respectively. For instance, graph "t2" shows the cumulative errors of the three decomposed levels. If every level has an error of less than 10 percent, the results should be less than 30 percent. Being less than 10 percent of each level can be monitored by Fig. 4. It shows that the error percentage is suitable up to the third level for small and medium dams. On the other hand, decomposition levels are suitable up to the fourth level in the large dams.

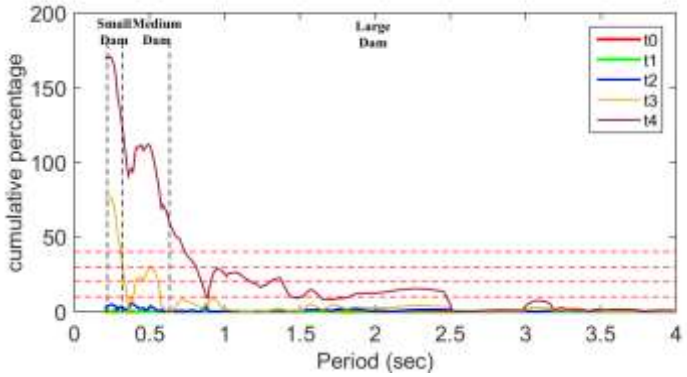

Figure 4. The percentage of cumulative error

4.2 Velocity-period

The ground velocity parameter has a close correlation with the intensity of the damage. It is also related to the energy transmitted to structures. Therefore, the velocity-period response spectrum of the ElCentro earthquake is studied here. Fig. 5 shows the velocity response spectrum for five levels of decomposition with the original one.

Fig. 5 is similar to Fig. 2 for different dams (i.e., small, medium, and large dams) and response spectrum (i.e., R1, R2, R3, R4, R5, Rx).

As the graph shows, the first three levels of decomposition can replace the primary response spectrum. This is because of the slight and acceptable difference between the results in small and medium dams. It can be concluded that the fourth level of decomposition cannot obtain purposes due to breaking the maximum difference limitation when compared with the acceleration-period curve (see Figs. 2 and 5).

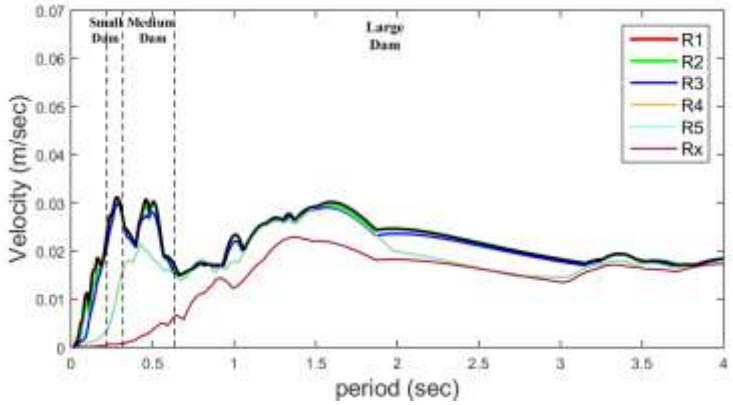

Figure 5. The velocity response spectrum of the ElCentro earthquake for 5 % damping ratio

The mean percentage difference between the decomposition level and the original signal in the second level is calculated for the small dams. The following results are shown in Table 6. From the results, it is clear that the first three levels have a slight difference (under 6 percent), and the remaining levels (i.e., fourth and fifth) have more than 50 percent disparity, which is not applicable.

Table 6: The mean response difference percentage for the small dams (0.22-0.318 sec)

Velocity-Period	Value
Mpd1 (%)	0.25
Mpd2 (%)	2.37
Mpd3 (%)	5.02
Mpd4 (%)	62.18
Mpd5 (%)	97.62

The same analysis is performed for the medium dam, and the results are computed (see Table 7). In this type of dam, the results follow a similar pattern in the first three levels, and their percentage differences are under 6 percent. This amount is less than the corresponding values for the small dams. For these two dam types, the quantities are more than 10 percent

in the fourth and fifth levels of decomposition (23.04 and 83.06, respectively), which cannot be an appropriate option.

Table 7: The mean response difference percentage for the median dams (0.318-0.633 *sec*)

Velocity-Period	Value
Mpd1 (%)	0.27
Mpd2 (%)	1.37
Mpd3 (%)	5.91
Mpd4 (%)	23.04
Mpd5 (%)	83.06

This process has a different result for large dams, which is shown in Table 8. Three decomposition levels have a percentage difference of less than 10 percent and can be replaced for optimization and design. However, the last two levels (fourth and fifth) are not suitable due to considerable disparity.

Comparing these types of dams reflect the fact that there is a similar pattern of differences in all types, and velocity has less flexibility and adaptability than acceleration.

Table 8: The mean response difference percentage for the large dams (>0.633 *sec*)

Velocity-Period	Value
Mpd1 (%)	0.22
Mpd2 (%)	0.50
Mpd3 (%)	2.43
Mpd4 (%)	10.93
Mpd5 (%)	22.10

At the next step, the percentage difference of each point between the decomposition level and the main one is shown in Fig. 6. It is clear from Fig. 6 that third levels of decomposition are less than the maximum error limit (the red horizontal line) in the small and medium dam. In comparison, the large dam has four acceptable levels under 10 percent (red horizontal line).

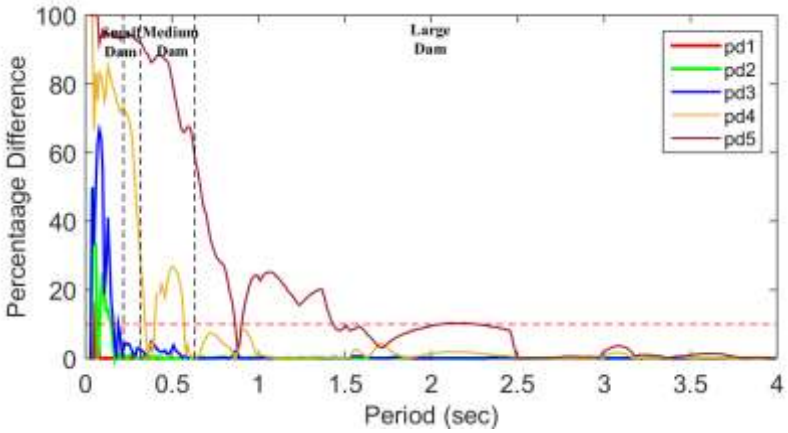

Figure 6. Percentage error for a point-by-point comparison with the original signal

Here, the percentage of cumulative difference for each level of decomposition is made to test the accuracy of the previous two steps (see Fig. 7). There are four horizontal lines in the graph to control the maximum error limit in the value of cumulative differences. These lines are 10, 20, 30, and 40 percent, respectively. For instance, graph "t2" shows the cumulative errors of the three decomposed levels. If every level has an error of less than 10 percent, the results should be less than 30 percent. Being less than 10 percent of each level can be monitored by Fig. 7. It shows that the error percentage is suitable up to the third level for small and medium dams. On the other hand, decomposition levels are suitable up to the fourth level in the large dams.

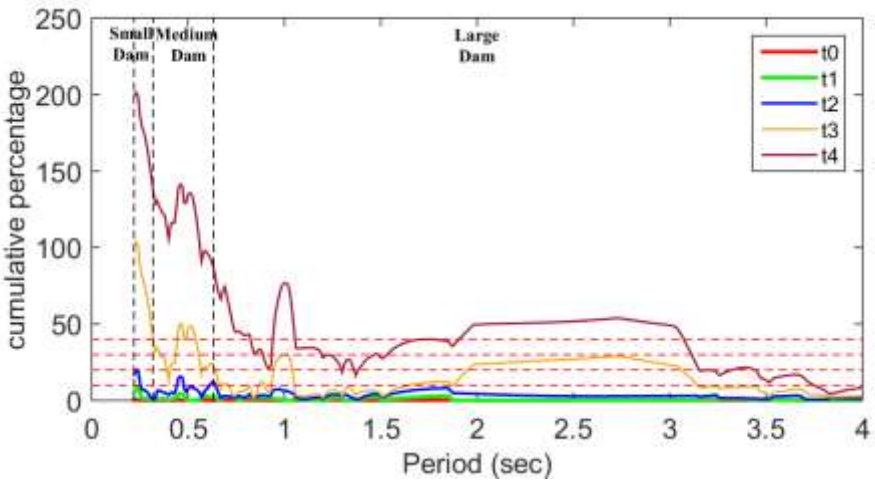

Figure 7. The percentage of cumulative error

4.2 Displacement-period

Since accelerations do not control structural damage during earthquakes, damage detection can be limited more effectively by monitoring displacements. For this purpose, the displacement-period response spectrum of the ElCentro earthquake is computed (see Fig. 8).

Fig. 8 is similar to Fig. 2 for different dams (i.e., small, medium, and large dams) and response spectrum (i.e., R1, R2, R3, R4, R5, Rx).

As the graph shows, the first three levels of decomposition can replace the primary response spectrum. This is because of the slight and acceptable difference between the results in small and medium dams. It can be concluded that the fourth level of decomposition cannot obtain purposes due to breaking the maximum difference limitation when compared with the acceleration-period curve (see Figs. 2 and 8).

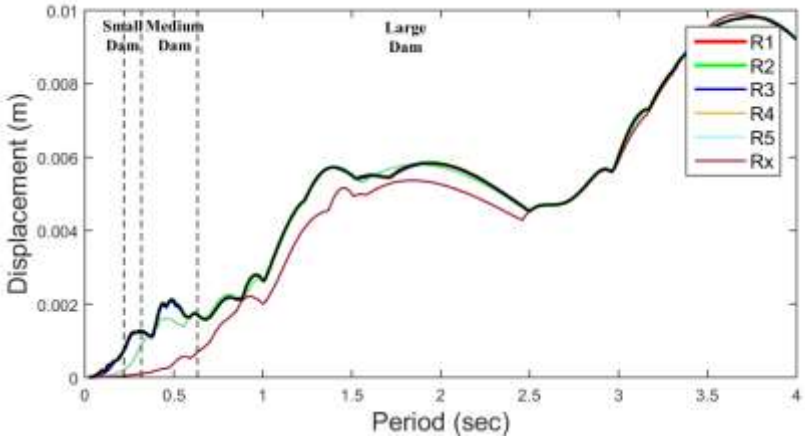

Figure 8. The displacement response spectrum of the ElCentro earthquake for 5 % damping ratio

The mean percentage discrepancy between each decomposition level and the original signal is calculated for the small dams (see Tabl 9). From the results, it is clear that the first three levels have a small difference (under 3 percent), and the remaining levels (i.e., fourth and fifth) have a noticeable disparity, which is not acceptable.

Table 9: The mean response difference percentage for the small dams (0.22-0.318 *sec*)

Displacement-Period	Value
Mpd1 (%)	0.08
Mpd2 (%)	0.6
Mpd3 (%)	2.54
Mpd4 (%)	47.15
Mpd5 (%)	92.40

The identical analysis is performed for the medium dams, and the results are computed and shown in Table 10. In this type of dam, the results follow a similar pattern in the first three levels, and their percentage differences are under 2 percent. This amount is less than the corresponding values for the small dams in the fourth and fifth levels. These values are more than 10 percent for these two types of dam (i.e., 12.22 and 75.52, respectively), which is not a good option.

Table 10: The mean response difference percentage for the median dams (0.318-0.633 *sec*)

Displacement-Period	Value
Mpd1 (%)	0.08
Mpd2 (%)	0.21
Mpd3 (%)	1.65
Mpd4 (%)	12.22
Mpd5 (%)	75.52

This process has a different result for large dams, which is shown in Table 11. All

decomposition levels have a percentage difference of less than 10 percent and can be replaced for optimization and design.

Comparing these dams reflects that large dams have complete flexibility and adaptability with the decomposition of acceleration.

At the next step, the percentage difference of each point between the decomposition level and the main one is found. Four out of five levels have an error of less than 10 percent, and the fifth level has an error above the maximum error value.

Table 11: The mean response difference percentage for the large dams (>0.633 *sec*)

Displacement-Period	Value
Mpd1 (%)	0.8
Mpd2 (%)	0.11
Mpd3 (%)	0.17
Mpd4 (%)	1.09
Mpd5 (%)	7.92

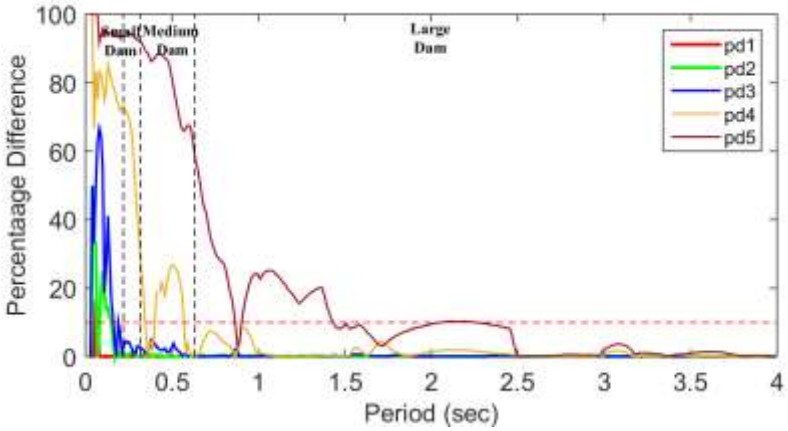

Figure 9. Percentage error for a point-by-point comparison with the original signal

Here, the percentage of cumulative difference for each level of decomposition is made to test the accuracy of the previous two steps (see Fig. 10). There are four horizontal lines in the graph to control the maximum error limit in the value of cumulative differences. These lines are 10, 20, 30, and 40 percent, respectively. For instance, graph "t3" shows the cumulative errors of the four decomposed levels. If every level has an error of less than 10 percent, the results should be less than 40 percent. Being less than 10 percent of each level can be monitored by Fig. 10. It shows that the error percentage is suitable up to the third level for small and medium dams. On the other hand, decomposition levels are suitable up to the fourth level in the large dams.

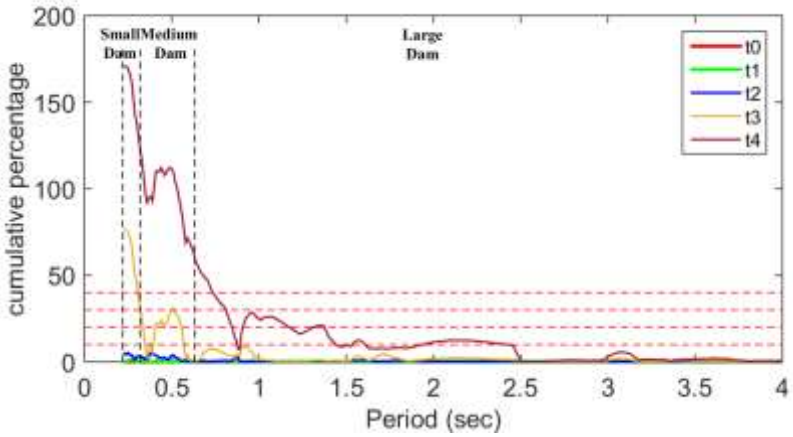

Figure 10. The percentage of cumulative error

5. CONCLUSIONS

The Strong Ground Motion records act as the input data for seismic analysis of structures. Since this data has errors caused by noise, wavelet transform decomposes noise and gives a more accurate examination of the signal. The function of the wavelet transform is to eliminate the noise from the signal, decrease the time of the calculation, and produce results closer to real ones.

The following results are obtained for the small, medium, and large dams with 5 percent damping ratio by investigation and analysis of some earthquakes, as well as comparison of primary earthquake response spectrum with response spectrum of decomposed levels in the domain of acceleration-time, velocity-time, displacement-time:

1. The difference between the acceleration response spectrum obtained by the main earthquake and the decomposed ones is less than ten for up to the third level of decomposition in the small and medium dams. This is valid up to the fourth level of decomposition for the large dams.
2. The difference between the velocity response spectrum obtained by the main earthquake and the decomposed ones is less than ten for up to the third level of decomposition in the small and medium dams. This is valid up to the fourth level of decomposition for the large dams.
3. The difference between the displacement response spectrum obtained by the main earthquake and the decomposed ones is less than ten for up to the third level of decomposition in the small and medium dams. This is valid up to the fourth level of decomposition for the large dams.
4. Large dams have more adaptability with decomposed levels of accelerations. They have fewer errors than small and medium dams.
5. Median dams have more adaptability with decomposed levels of accelerations. They have fewer errors than small dams.

This approach is taken for the study of the response spectrum of other structures. It helps the designer have an optimum design based on alternating the optimum level of

decomposition with the primary earthquake.

ACKNOWLEDGMENT: The authors would like to appreciate the use of the computational clusters of the HPC center (Shahr–e–Kord University, Iran) to complete this work.

REFERENCES

1. Islam A, Jameel M, Ahmad S I, Salman F, Jumaat MZ. Engendering earthquake response spectra for Dhaka region usable in dynamic analysis of structures, *Sci Res Essays* 2011; **6**(16): 3519-30.
2. Derras B, Bekkouche A. Use of the artificial neural network for peak ground acceleration estimation, *Lebanese Sci J* 2011; **12**(2): 101-15.
3. Günaydın K, Günaydın A. Peak ground acceleration prediction by artificial neural networks for northwestern Turkey, *Mathemat Prob Eng* 2008; **2008**:1-20.
4. Linkimer L. Relationship between peak ground acceleration and modified Mercalli intensity in Costa Rica, *Revista Geológica de América Central* 2008; **38**: 81-94.
5. Trombetti T, Silvestri S, Gasparini G, Righi M, Ceccoli C. Correlations between the displacement response spectra and the parameters characterising the magnitude of the ground motion, In *14th World Conference on Earthquake Engineering* 2008, Beijing, China.
6. Omine H, Hayashi T, Yashiro H, Fukushima S. *Seismic risk analysis method using both PGA and PGV*, In *14th World Conference on Earthquake Engineering*. 2008. Beijing, China.
7. Gandomi AH, Alavi AH, Mousavi M, Tabatabaei SM. A hybrid computational approach to derive new ground-motion prediction equations, *Eng Applicat Artific Intell* 2011; **24**(4): 717-32.
8. Esposito S, Iervolino I, Silvestri F, D'Onofrio A, Santo A. Seismic risk analysis of lifelines: Preliminary results for the case-study of l'aquila enel rete gas, In *15th World Conference of Earthquake Engineering* 2012. Lisbon, Portugal.
9. Ghodrati Amiri G, Mahtabi MJ, Razavian Amrei SA. Seismic velocity and displacement hazard assessment for Tehran, including site effects, *Asian J Civil Eng* 2012; **13**(3): 331-51.
10. Song S, Heaton T H. Prediction of collapse from PGV and PGD, In *15th World Conference of Earthquake Engineering* 2012, Lisbon, Portugal.
11. Corchete V. The analysis of accelerograms for the earthquake resistant design of structures, *Int J Geosci* 2010; **1**(1): 32-7.
12. Segou M, Voulgaris N. Proschema: A Matlab application for processing strong motion records and estimating earthquake engineering parameters, *Comput Geosci* 2010; **36**(7): 977-86.
13. Yu Z, Abma R, Etgen J, Sullivan C. Attenuation of noise and simultaneous source interference using wavelet denoising, *Geophysic* 2017; **82**(3): 179-90.
14. Heidari A, Majidi N. Earthquake acceleration analysis using wavelet method, *Earthq Eng Eng Vib* 2021; **20**(1): 113-26.

15. Heidari A, Raeisi J, Pahlavan Sadegh S. A new method for calculating earthquake characteristics and nonlinear spectra using wavelet theory, *J Rehabilit Civil Eng* 2020; **8**(1): 50-62.
16. Kamgar R, Dadkhah M, Naderpour H. Seismic response evaluation of structures using discrete wavelet transform through linear analysis, *Struct* 2021; **29**: 863-82.
17. Kamgar R, Majidi N, Heidari A. Wavelet-based decomposition of ground acceleration for efficient calculation of seismic response in elastoplastic structures, *Period Polytech Civil Eng* 2021; **65**(2): 409-24.
18. Kamgar R, Tavakoli R, Rahgozar P, Jankowski R. Application of discrete wavelet transform in seismic nonlinear analysis of soil–structure interaction problems, *Earthq Spectra* 2021; **37**(3): 1980-2012.
19. Kumar M, Pandit S. Wavelet transform and wavelet based numerical methods: an introduction, *Int J Nonlin Sci* 2012; **13**(3): 325-45.
20. Yaghmaei-Sabegh S, Ruiz-García J. Nonlinear response analysis of SDOF systems subjected to doublet earthquake ground motions: A case study on 2012 Varzaghan–Ahar events, *Eng Struct* 2016; **110**: 281-92.
21. Heidari A, Raeisi J, Kamgar R. Application of wavelet theory in determining of strong ground motion parameters, *Int J Optim Civil Eng* 2018; **8**(1): 103-15.
22. Heidari A, Raeisi J, Kamgar R. The application of wavelet theory with denoising to estimate the parameters of earthquake, *Sci Iran* 2021; **28**(1): 49-64.
23. Kaveh A. *Optimum Design of Multi-span Composite Box Girder Bridges Using Cuckoo Search Algorithm*, Springer International Publishing, Cham, 2017.
24. Kaveh A, Maniat M, Naeini MA. Cost optimum design of post-tensioned concrete bridges using a modified colliding bodies optimization algorithm, *Adv Eng Softw* 2016; **98**:12-22.
25. Kaveh A, Motesadi Zarandi MM. Optimal design of steel-concrete composite I-girder bridges using three meta-heuristic algorithms, *Period Polytech Civil Eng* 2019; **63**(2): 317-37.
26. Rahmani F, Kamgar R, Rahgozar R. Optimum design of long-term deflection in segmented prestress bridges by considering the effects of creep and shrinkage, *Int J Optim Civil Eng* 2020; **10**(2): 315-31.
27. Kaveh A, Ilchi Ghazaan M, Saadatmand F. Colliding bodies optimization with Morlet wavelet mutation and quadratic interpolation for global optimization problems, Engineering with Computers 2021. DOI: 10.1007/s00366-020-01236-z.
28. Kaveh A, Mahdavi VR. Generation of endurance time acceleration functions using the wavelet transform, *Int J Optim Civil Eng* 2012; **2**(2): 203-19.
29. Kaveh A, Mahdavi VR. A new method for modification of ground motions using wavelet transform and enhanced colliding bodies optimization, *Appl Soft Comput* 2016; **47**: 357-69.
30. ASCE7-10. *Minimum Design Loads for Buildings and Other Structures*, The American Society of Civil Engineers, ASCE, USA, 2010.